J. Mol. Model. **1998**, *4*, 355 – 365

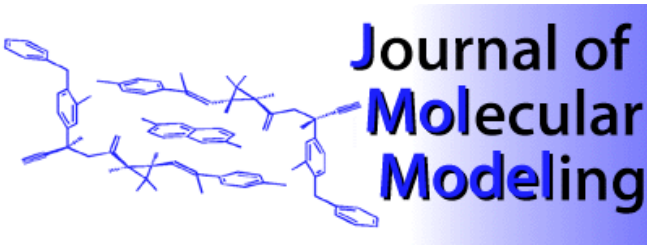

FULL PAPER

The Important Role of Active Site Water in the Catalytic Mechanism of Human Carbonic Anhydrase II - A Semiempirical MO Approach to the Hydration of CO_2†

Michael Hartmann[1,2], Kenneth M. Merz, Jr.[3], Rudi van Eldik[2], and Timothy Clark[1]

[1]Computer-Chemie-Centrum, Universität Erlangen-Nürnberg, Nägelsbachstr. 25, D-91052 Erlangen,Germany. Tel: +49-9131-8522948; Fax:+49-9131-8526565. E-mail: clark@organik.uni-erlangen.de

[2]Institut für Anorganische Chemie, Universität Erlangen-Nürnberg, Egerlandstr.1, D-91058 Erlangen, Germany.

[3]Department of Chemistry, 152 Davey Laboratory, The Pennsylvania State University, University Park, Pennsylvania 16802, USA.

Received: 4 August 1998 / Accepted: 2 October 1998 / Published: 24 November 1998

Abstract The approach of CO_2 to a series of active site model complexes of human carbonic anhydrase II (HCAII) and its catalytic hydration to bicarbonate anion have been investigated using semiempirical MO theory (AM1). The results show that direct nucleophilic attack of zinc-bound hydroxide to the substrate carbon occurs in each model system. Further rearrangement of the bicarbonate complex thus formed *via* a rotation-like movement of the bicarbonate ligand can only be found in active site model systems that include at least one additional water molecule. Further refinement of the model complex by adding a methanol molecule to mimic Thr-199 makes this process almost activationless. The formation of the final bicarbonate complex by an internal (intramolecular) proton transfer is only possible in the simplest of all model systems, namely $\{[Im_3Zn(OH)]^+ \cdot CO_2\}$. The energy of activation for this process, however, is 36.8 kcal·mol^{-1} and thus too high for enzymatic catalysis. Therefore, we conclude that within the limitations of the model systems presented and the level of theory employed, the overall mechanism for the formation of the bicarbonate complex comprises an initial direct nucleophilic attack of zinc-bound hydroxide to carbon dioxide followed by a rotation-like rearrangement of the bicarbonate ligand *via* a penta-coordinate Zn^{2+} transition state structure, including the participation of an extra active site water molecule.

Keywords Human carbonic anhydrase II, Semiempirical MO theory, AM1, Enzyme catalysis

†M.J.S. Dewar, in memoriam

Correspondence to: R. van Eldik and T. Clark

Introduction

The human carbonic anhydrases (HCAs) are a family of at least seven known genetically-distinct enzymes (HCAI - HCAVII), whose essential physiological function is to catalyse the hydration of CO_2 and its reverse, the dehydration of HCO_3^- (equation 1). [1-3] The former (forward) reaction dominates above pH 7, whereas the latter (backward) reaction is favoured below pH 7. [1-3]

$$H_2O + CO_2 \rightleftharpoons H^+ + CO_3^- \quad (1)$$

HCAs, of which three isoenzymes have maximal turnover numbers at 25°C of 10^5 (HCAI), 10^6 (HCAII), and 10^4 (HCAIII), comprise one of the most efficient groups of enzymes. [1,4] The nature of their active sites is highly conserved among all active isoenzymes and is of great interest. [1-3,5] The active site of HCAII has a catalytically required Zn^{2+} ion bound at the bottom of a 15 Å deep solvent-exposed cavity. The metal ion is coordinated in a slightly distorted tetrahedral geometry by three N atoms of His-94, -96 and -119 and by a water (pH<7) or a hydroxide (pH>7). [1-3,6] Further key features of the active site cavity that appear to be important in the enzymatic catalysis are hydrogen bonds between zinc-bound ligands and Thr-199, between Thr-199 and Glu-106, and among a group of up to eight water molecules. [1-3,6-8] This latter hydrogen bond network has been proposed to operate as a proton shuttle towards the bulk solution involving the neighbouring His-64. [1,8]

The most widely accepted catalytic mechanism for the enzymatic activity of carbonic anhydrase, first proposed by Davis and Coleman, [9] is generally considered to comprise three distinct mechanistic steps. First, deprotonation of the zinc-bound water yields the catalytically active zinc-hydroxo species. His-64 and active site water molecules are thought to act as a proton shuttle in order to release the proton to the bulk solution. [1,8] Second, the hydration of CO_2 leads to the formation of a zinc-bicarbonate species. Two alternative mechanisms have been proposed to explain the details of the formation of the final bicarbonate complex (Scheme 1). [2,3,10] In the first mechanism, following the direct nucleophilic attack of zinc-bound hydroxide onto the carbon dioxide substrate, there is an internal proton transfer between two oxygens of the bicarbonate ligand (the Lipscomb-mechanism), [3,10] whereas the second mechanism proposes a rotation-like movement of the bicarbonate ligand, yielding the desired bicarbonate complex (the Lindskog-mechanism). [2] The third step in the overall catalysis of HCAII involves the substitution of bicarbonate by water, which yields the starting zinc-aqua species. The loss of bicarbonate is thought to be mediated by active site water. [8]

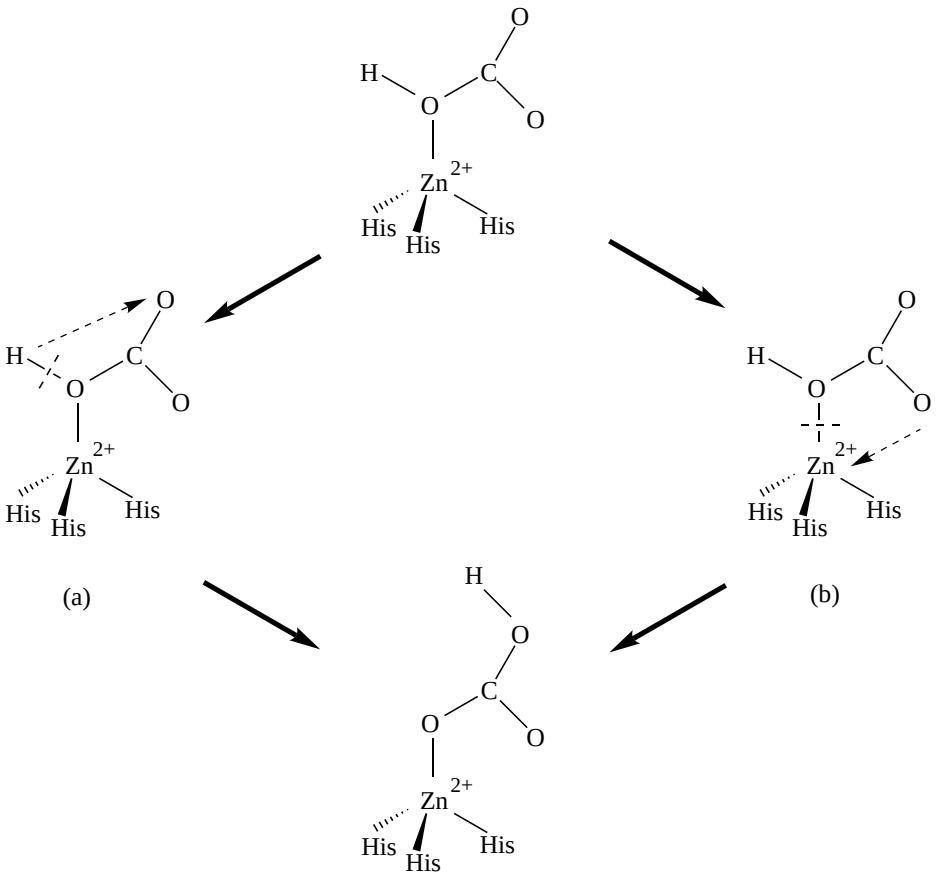

Scheme 1 *Two alternative pathways for the formation of the bicarbonate complex. Internal proton transfer (a) according to Lipscomb [3,10] and rotation-like rearrangement (b) proposed by Lindskog [2]*

In this study, we focus on the second step of the catalytic cycle, namely the formation of the bicarbonate complex and hence the preferred binding mode of the bicarbonate ligand. In doing so, we follow the work of Dewar et al., [8] which we consider to be an important contribution to our understanding of the mechanism of bicarbonate formation in HCAII-catalysis. [1-3,8,10-18] First we focus on the reaction (i.e approach of CO_2 and subsequent rearrangement within the coordination sphere of Zn^{2+}) between the simplest model complex $[Zn(Im)_3OH]^+$ (Im = Imidazole) and carbon dioxide. Second, in order to analyse the role of active site water in the formation of the bicarbonate complex, we extend our model by one additional water molecule. Further modification of the active site model considers catalytically important side chain models, such as methanol for Thr-199. The effect of these additional residues in active site models on the overall reaction mechanism will be discussed and differences in the energetic and structural details will be highlighted.

Methodology

Active site model systems

In order to be able to define the roles of active site water and side chains exactly, we started with the smallest possible model that mimics the HCAII active site realistically. This model uses imidazoles instead of the histidine ligands. It has been shown elsewhere [8,19,20] that this simplification is justified. In addition the RMSD value of 1.09 Å obtained by superimposing the AM1-optimised geometry of the $[Im_3Zn]^{2+}$ model complex on the corresponding structure taken from the X-ray structure of HCAII (Scheme 2) [21] further supports the use of this complex as active site model for HCAII.

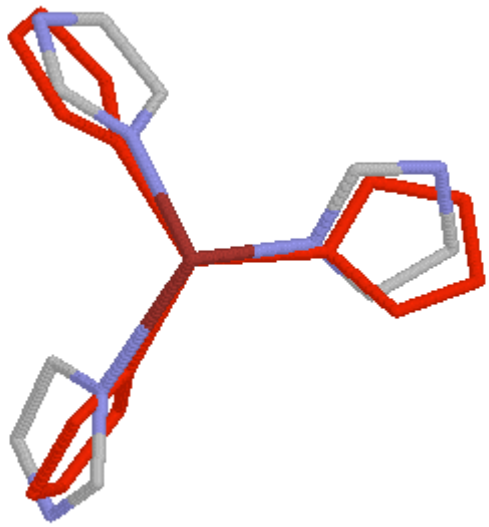

Scheme 2 *Optimised active site model $[Im_3Zn]^{2+}$ (CPK colours) and active site taken from X-ray structure (red, Brookhaven Database ID: 12CA). The RMSD value with respect to the heavy atoms is 1.09 Å*

Therefore, all active site models consist at least of an $[Im_3ZnOH]^+$-core fragment, which binds the CO_2 substrate. Further, modified model systems include active site water and a methanol to mimic the influence of the Thr-199 side chain. The active site models studied are thus: $\{[Im_3ZnOH]\cdot CO_2\}^+$, $\{[Im_3ZnOH]\cdot H_2O\cdot CO_2\}^+$, and $\{[Im_3ZnOH]\cdot H_2O\cdot CH_3OH\cdot CO_2\}^+$.

Computational details

AM1 [22] calculations were performed on SGI Indigo2 workstations and on a SGI Power Challenge using the semi-empirical program package VAMP 7.0. [23] All calculations used the standard AM1 parameters for C, H, O, N, [22] and Zn. [24] Optimisations of minima were performed using the default EF algorithm, [25] whereas transition state optimisations either used Powell's NS01A [26] or non-linear least squares (NLLSQ) methods. [27] Suitable starting geometries for transition state optimisations were obtained by one- or two-dimensional searches with fixed geometrical parameters using the reaction coordinate method with appropriate geometrical variables as reaction coordinates. [28] All stationary points found were characterised by diagonalisation of the AM1-calculated force-constant matrix and additionally verified by intrinsic reaction coordinate calculations (IRC). [29] All geometries were optimised fully with no symmetry constraints (i.e. in C_1 symmetry).

Results and discussion

In general, we will indicate the distance between CO_2 and the active site model by means of two structural parameters, denoted r(CO···Zn) and r(C···OZn) (Table 1). The first represents the shortest distance between CO_2 oxygen and Zn^{2+} and thus indicates whether or not CO_2 is prone to coordinate directly to the metal centre of the active site model complexes. The second measures the distance between CO_2 carbon and zinc-bound hydroxide oxygen and therefore the overall progress of the CO_2 approach to the active site model complex. Transition state structures shown in Figures 1-3 are abbreviated according to the number of the structure of their respective reactant complex and the abbreviation "TS". Videos 1-3 are animations of each reaction sequence shown in Figures 1-3, respectively. The individual structures for these videos were taken directly from the IRC calculations performed in order to verify that the reactant and product complexes are indeed connected by the proposed transition state structures. [30]

Table 1 *Selected structural parameters r(CO···Zn) and r(C···OZn) given in [Å]. For a description of these bond distances refer to the text. Heats of formation ΔH_f in [kcal·mol^{-1}] obtained using the AM1-hamiltonian*

Structure	r(CO···Zn)	r(C···OZn)	ΔH_f
CO_2	–	–	-79.9
H_2O	–	–	-59.3
CH_3OH	–	–	-57.1
1	–	–	242.2
2	4.21	2.37	161.2
2TS	3.66	1.80	165.4
3	3.63, 3.92	1.49	161.5
3TS	3.62, 3.92	1.39	198.3
4	4.44	2.43	160.2
4TS	3.89, 4.00	1.79	164.9
5	3.18	1.30	140.3
5TS	3.25	1.30	147.1
6	3.28	1.29	140.2
7	4.39	2.39	93.0
7TS	3.81	1.86	96.3
8	3.36	1.45	89.0
8TS	2.94	1.44	89.4
8TS2	3.82, 3.78	1.31	110.3
9	2.10	1.38	77.9
9TS	2.11	1.37	78.1
10	2.11	1.36	75.6
11	4.39	2.34	31.1
11TS	3.81	1.83	34.3
12	3.30	1.46	28.1
12TS	3.15	1.45	28.2
13	2.11	1.38	15.9

The {[Im_3ZnOH]$^+$·CO_2} active site model complex

Approach of CO_2 Optimised geometries and relative energies, selected structural data and calculated heats of formation of the complexes used for modelling the approach of the CO_2 substrate to the active site model complex **1** are shown in Figure 1 and Table 1, respectively. The optimised geometry of reactant **1**, which is perfectly in accord with analogous structures reported by others, [8,12,13] shows Zn-N bond lengths of 2.1 Å and a Zn-O distance of 1.97 Å. In general, two alternative energetically almost equivalent pathways were found for the reaction between CO_2 and **1**. In the first mechanism (Figure 1a) the initial van der Waals-complex **2** has CO_2 loosely bound to **1** by two hydrogen bonds between one carbon dioxide oxygen and two imidazole hydrogens. The gain in energy on going from **1** to **2** is 1.1 kcal·mol^{-1}. For van der Waals-complex **2**, the r(CO···Zn) and r(C···OZn) bond distances were calculated to be 4.21 Å and 2.37 Å, respectively. Further approach of the CO_2 substrate leads to the transition state structure **2TS**, which is 4.2 kcal·mol^{-1} higher in energy than **2**. The r(CO···Zn) and r(C···OZn) distances are shortened to 3.66 Å and 1.80 Å, respectively, indicating that CO_2 does not penetrate the first coordination sphere of Zn^{2+} on nucleophilic attack by the hydroxide oxygen, as also found for CPA and LADH. [20] Passing through the transition state structure **2TS** yields the *precursor* bicarbonate complex **3**, which is 3.9 kcal·mol^{-1} lower in energy than the preceding transition state structure. Interestingly, the CO_2 rearranges slightly in order to make two hydrogen bonds, each of them now being between one carbon dioxide oxygen and one imidazole hydrogen. The carbon dioxide oxygens are still too far away from the zinc centre for direct coordination. This is indicated by r(CO···Zn) values of 3.63 Å and 3.92 Å, respectively. The (C···OZn) contact, calculated to be 1.49 Å is, however, surprisingly short but in line with the results reported earlier.[8,20]

Further search for suitable mechanisms for the reaction of CO_2 with **1** yielded an alternative pathway (Figure 1b), which differs from the first in its CO_2 orientation on approaching **1**. The van der Waals complex **4** thus formed shows only one hydrogen bond between a CO_2 oxygen and imidazole hydrogen. The gain in energy for this step is 2.1 kcal mol^{-1}, making complex **4** more stable than **2** by 1.0 kcal·mol^{-1} despite the fact that only one hydrogen bond is formed. This, however, implies that the repulsive interaction of one imidazole hydrogen and the zinc-bound hydroxide hydrogen in structure **2** cannot be compensated completely by two hydrogen bonds. Thus, only one hydrogen bond between the CO_2 oxygen and an imidazole hydrogen is formed with the zinc-bound hydroxide hydrogen now located between two hydrogens of two imidazole ligands. The r(CO···Zn) distance is 4.44 Å, whereas r(C···OZn) is 2.43 Å. Further approach of CO_2 leads to transition state **4TS**, in which the CO_2 is reoriented. Now two hydrogen bonds (between each CO_2 oxygen and one imidazole) are formed. The distances of the two CO_2 oxygens are 3.89 Å and 4.00 Å, indicating that there is no tendency for direct CO_2 coordination to Zn^{2+}. The r(C···OZn) bond length is shortened to 1.79 Å in this transition state. The energy of activation on going from **4** to **3** is +4.7 kcal·mol^{-1} and thus only 0.5 kcal·mol^{-1} higher than for the analogous step shown in Figure 1a. The overall reaction energy for the formation of **3** according to Figure 1b was calculated to be 1.3 kcal·mol^{-1} and is thus more endothermic by 1.0 kcal·mol^{-1} than the alternative reaction shown in Figure 1a. Again, the *precursor* bicarbonate complex **3** is found on following the reaction coordinate further. IRC calculations show that **3** is indeed the common product yielded by transition states **2TS** and **4TS**.

Binding Mode of HCO_3^- In principle, starting from the *precursor* bicarbonate complex **3**, two mechanisms, those proposed by Lipscomb (internal proton transfer) [3,10] and Lindskog (bicarbonate rotation), [2] have been suggested for the formation of the final bicarbonate complex. In the final catalytic step of HCAII, the bicarbonate complex undergoes substitution by water in order to release the HCO_3^-ligand. In the first mechanism, bicarbonate acts as a monodentate ligand and the internal proton transfer occurs without a change in the coordination number of Zn^{2+}. This mechanism could

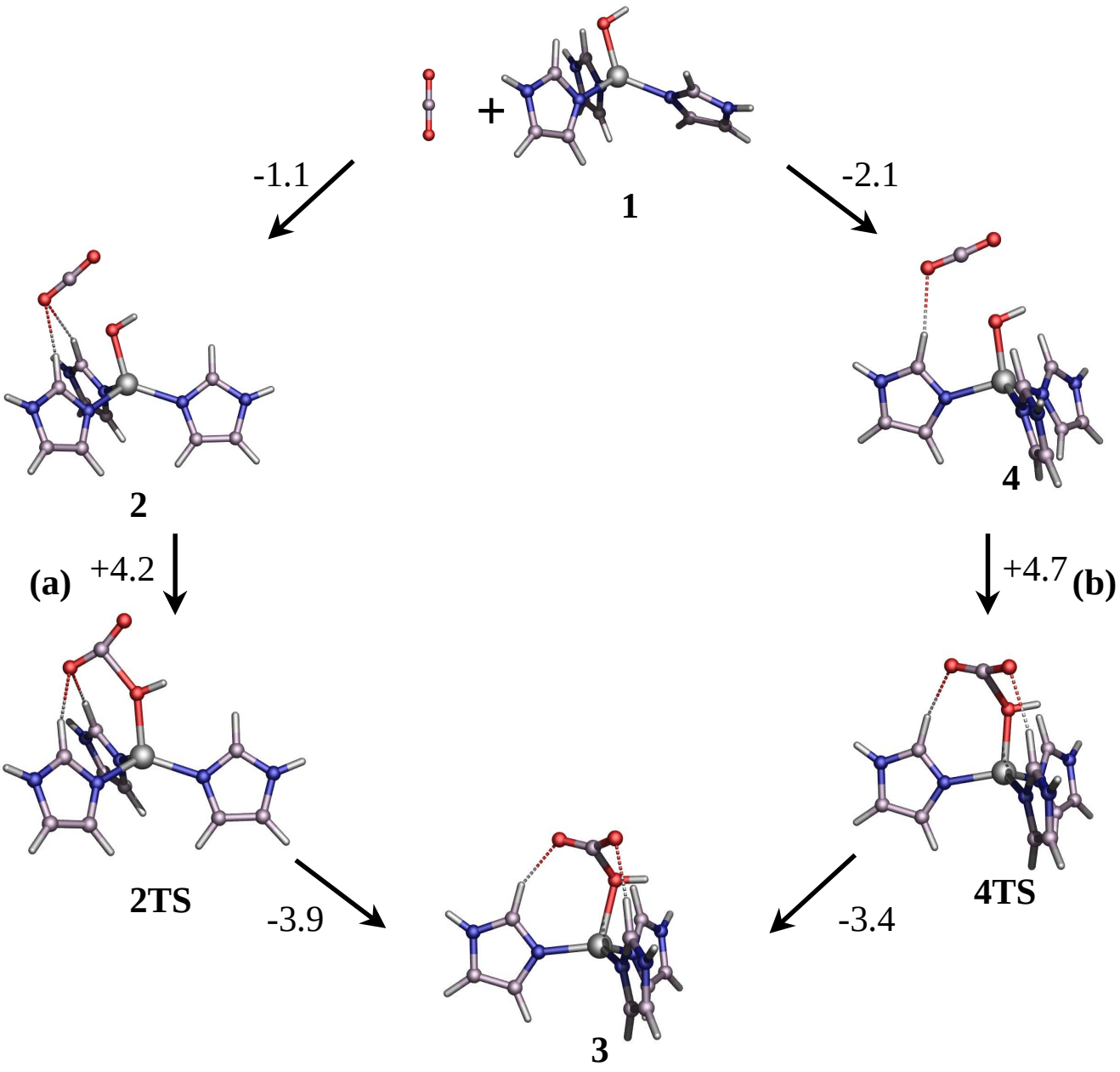

Figure 1 *Approach of CO_2 to the active site model complex $[Im_3ZnOH]^+$. Relative energies are given in [kcal·mol^{-1}]. For selected structural data and heats of formation see Table 1. Two possible reaction paths are shown: CO_2 initially having two (a) or one (b) hydrogen bonds to imidazole hydrogens*

be reproduced within our simplified model system. Figure 2 and Table 1 summarise the resulting energetic and structural details for a Lipscomb-like mechanism. The transition state **3TS** for internal proton transfer is 36.8 kcal·mol^{-1} higher in energy than the preceding complex **3**. Both r(CO···Zn) bond lengths of **3TS** are equal to the equivalent distances in **3**, implying that the proton transfer does not affect the coordination geometry of Zn^{2+} and thus ruling out any tendency of CO_2 to act as a bidentate ligand in this model system. The total energy of activation is used solely for the transfer of the proton from the zinc bound HCO_3^- oxygen to the carbon bound HCO_3^- oxygen. Passing this transition state along the

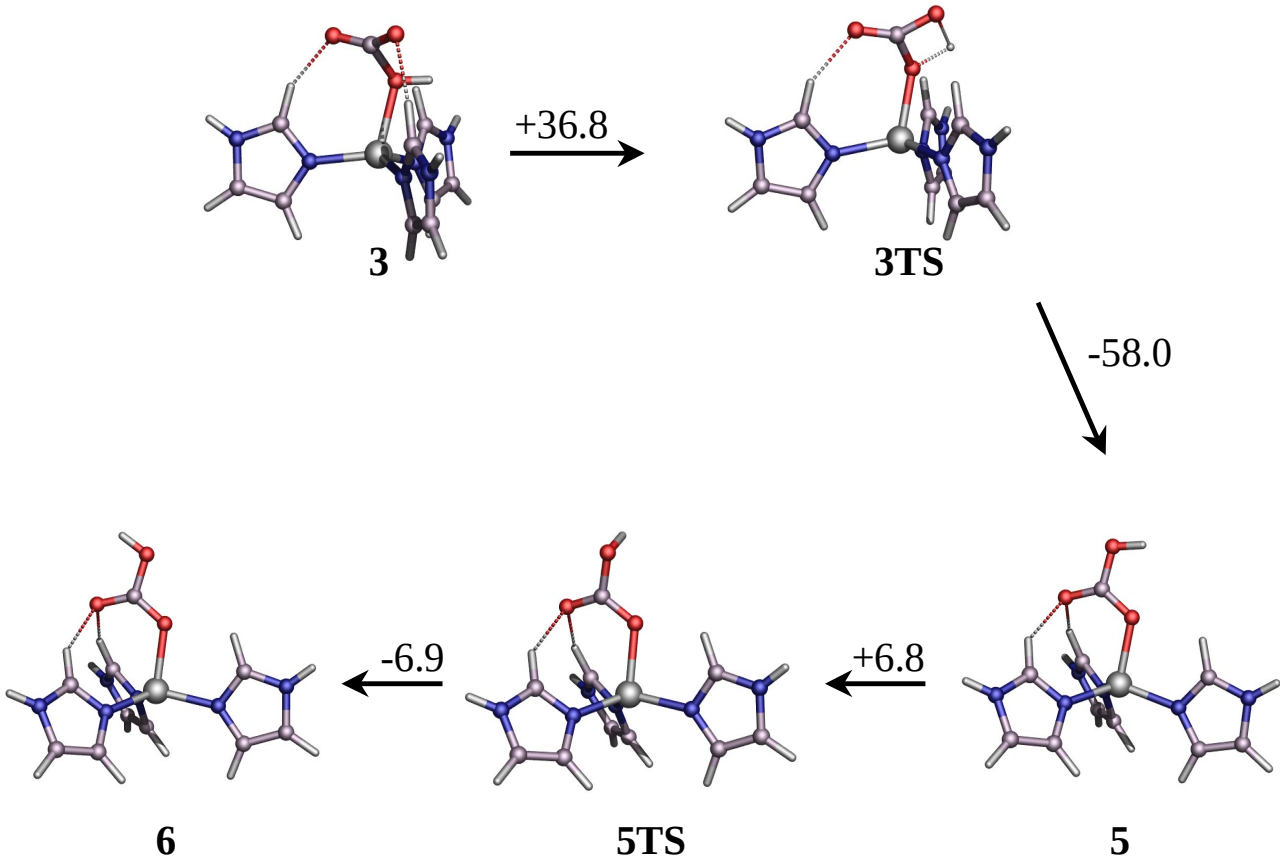

Figure 2 *Internal proton-transfer calculated using AM1 and tight convergence criteria for energies and gradients. Relative energies are given in [kcal·mol^{-1}] and selected structural parameters and heats of formation are summarised in Table 1*

reaction coordinate yields complex **5**, which is more stable than the preceding transition state by 58.0 kcal·mol^{-1}. Further rotation around the C–O bond of the bicarbonate ligand first leads to transition state **5TS** and finally to the most stable isomer of the bicarbonate complex **6**. The energy of activation for this "isomerisation" was calculated to be 6.8 kcal·mol^{-1}, with a reaction energy of –0.1 kcal·mol^{-1}. Although the overall mechanism seems reasonable from a theoretical point of view, the calculated energy of activation for the internal proton transfer is too high for an enzymatic reaction. In spite of the results reported elsewhere [8], no evidence for a transition state structure simulating the second, Lindskog-like mechanism, characterised by a five-fold coordinated Zn^{2+} centre in the transition state structure, could be found. Although transition state optimisations aimed at such a structure initially tended to yield a five-fold coordinated Zn^{2+} complex, they invariably led to complexes of type **3** and **5**. This behaviour is even more pronounced when tight convergence criteria for energies and gradients are used. Therefore, we conclude that within this model system and the limitations of the level of theory used, the existence of a Lindskog-like transition state structure seems unlikely and that this active site model complex is not sophisticated enough to yield reasonable energies of activation for the final bicarbonate complex, which is formed *via* an internal proton transfer. The complete reaction sequence - Figure 1a followed by the internal proton-transfer in Figure 2 - is animated in Video 1.

The {[Im$_3$ZnOH]$^+$·H$_2$O·CO$_2$} active site model complex

The shortcomings of the model system {[Im$_3$ZnOH]$^+$·CO$_2$} show the necessity of further improvements of the active site model. It was therefore extended by an additional so-called "deep" water molecule. The effect on the overall mechanism, i.e. on the approach of CO_2 to the active site and the formation of the final bicarbonate complex is shown in Figure 3. Selected structural parameters and heats of formation are summarised in Table1. As in the first model system, there is no evidence for direct coordination of CO_2 to Zn^{2+}. The interaction of **1** with CO_2 and H_2O yields the van der Waals-complex **7**, which shows a well established hydrogen bond pattern between the three reactants. Comparison with the analogous steps in the first model system (Figure 1) reveals

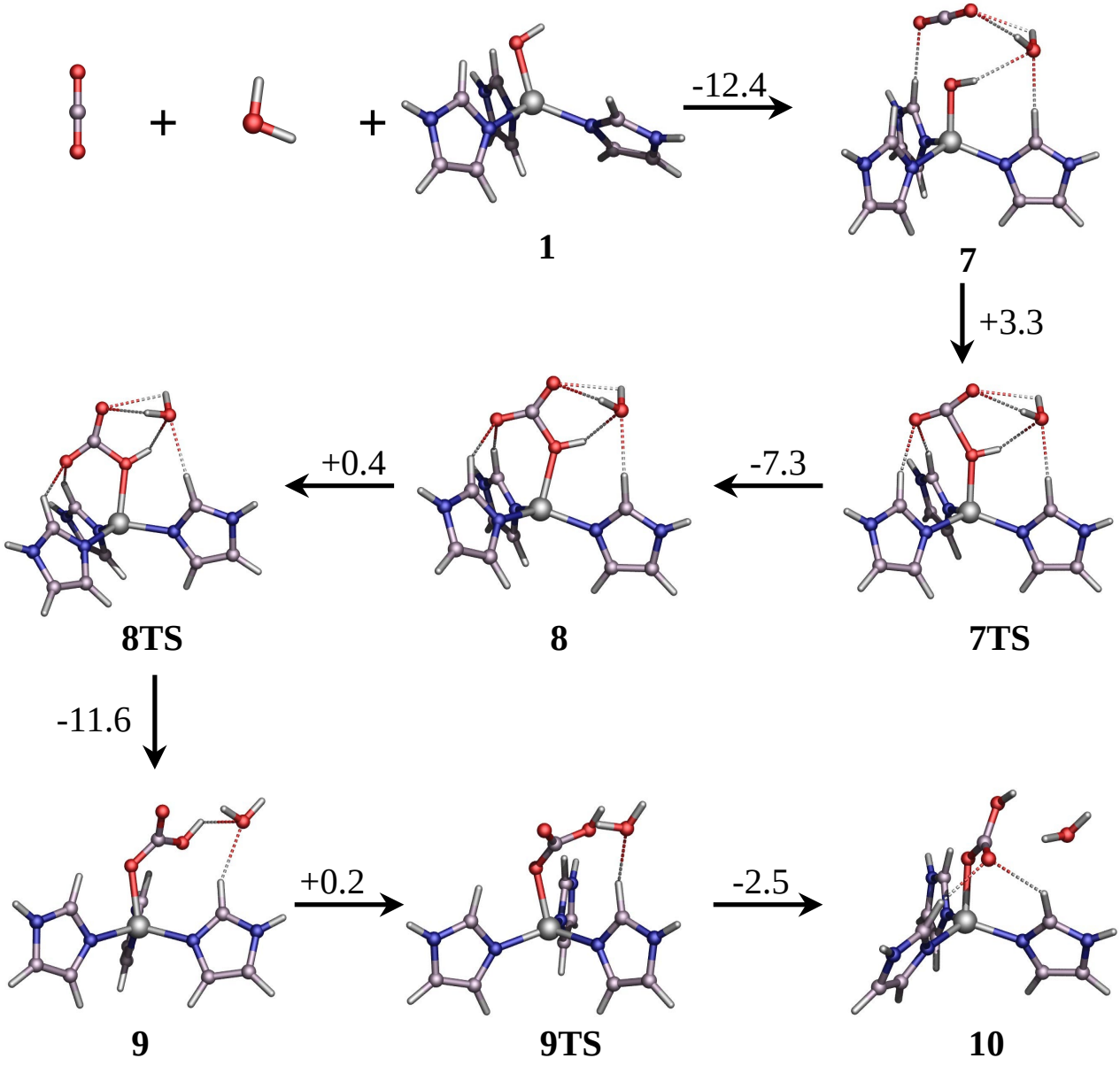

Figure 3 *Formation of the bicarbonate complex* via *a five-fold transition state structure. Relative energies are given in [kcal·mol^{-1}]. Selected structural parameters and the heats of formation obtained for each complex are listed in Table 1*

that the formation of **7** is more exothermic by 11.3 kcal·mol^{-1} than for **2,** and 10.3 kcal·mol^{-1} compared to **4**. Further approach of CO_2 to the active site leads to the formation of transition state structure **7TS**, which gives the *precursor* bicarbonate complex **8**. The energy of activation was calculated to be 3.3 kcal·mol^{-1} and is thus almost 1 kcal·mol^{-1} lower than for the equivalent reaction in the absence of a water molecule (first model system). The reaction energy for the formation of **8** is –4.0 kcal·mol^{-1}. The calculated r(CO···Zn) distance of **7TS** is 3.81 Å, whereas it is 3.36 Å in **8**, indicating that no direct coordination of CO_2 oxygen to Zn^{2+} occurs. The next step in the reaction sequence involves the rearrangement of the bicarbonate ligand, which was found to occur by a rotation-like movement of HCO_3^-, rather than an internal proton-transfer. The energy of activation to reach transition state structure **8TS** is only 0.4 kcal·mol^{-1}. The r(CO···Zn) distance, which indicates whether coordination of CO_2 oxygen to Zn^{2+} occurs, is 2.94 Å, so that rotation of the bicarbonate ligand *via* a five-fold coordinated Zn^{2+}-ion can occur in principle. This is due to the active site water molecule, which mediates and thus facilitates the rotation of the HCO_3^- ligand by means of hydrogen bonds. Vibrational analysis of **8TS** gives one imaginary mode showing the movement of a CO_2 oxygen to the metal centre. Passing this transition state fur-

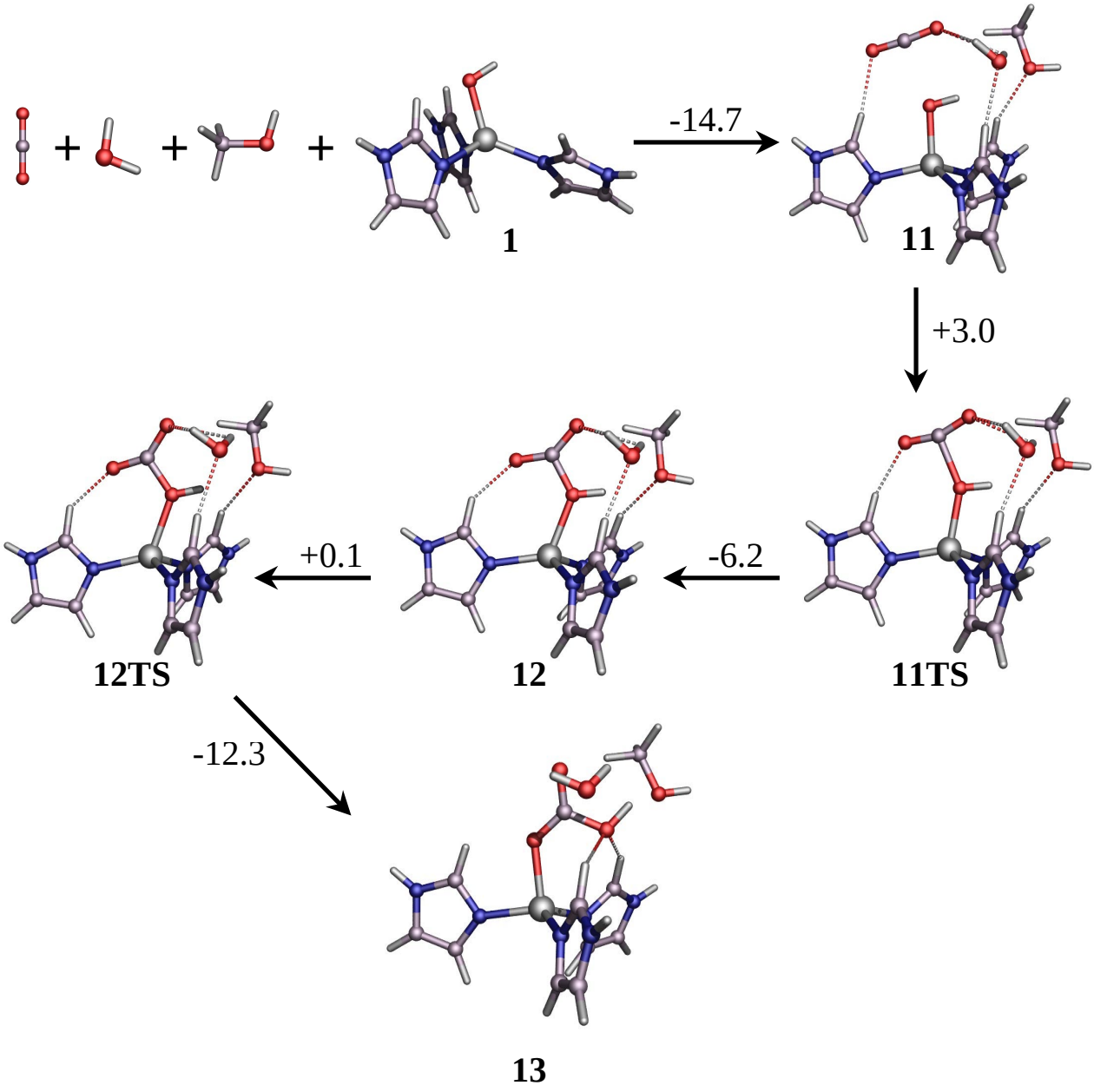

Figure 4 *Formation of bicarbonate* via *rotation-like movement of the HCO_3^- ligand. For selected structural data and heats of formation see Table 1. An additional methanol molecule is used in order to mimic the influence of the Thr-199 side chain*

ther along the reaction path leads to the first bicarbonate complex **9**, in which most of the hydrogen bond pattern is lost. However, this reaction step is still exothermic with a gain in energy of 11.6 kcal·mol^{-1}. The former r(CO···Zn) distance is now shortened to 2.10 Å, indicating a true chemical bond between a CO_2 oxygen and Zn^{2+}. Further rearrangement of the HCO_3^- ligand *via* transition state **9TS** yields the second, final bicarbonate complex **10**, which again shows hydrogen bonds between two imidazole hydrogens and one bicarbonate oxygen. The energy of activation for forming these hydrogen bonds is once more only 0.2 kcal·mol^{-1}, whereas the reaction energy on going from **9** to **10** is -2.3 kcal·mol^{-1}. Therefore the overall mechanism shown in Figure 3 represents a Lindskog-like formation of the bicarbonate complex with the highest energy barrier of 3.3 kcal·mol^{-1} for the formation of a *precursor* bicarbonate complex. The activation energy for the rotation-like rearrangement of the bicarbonate ligand mediated by "deep" water is only 0.4 kcal·mol^{-1}, so that this process is almost activationless. Thus, the addition of just one water molecule to the first active site model com-

plex leads to a model system that from an energetic and structural point of view mimics enzymatic catalysis of HCAII reasonably. Note, however, that the mobility of the water molecule in the real active centre is reduced significantly due to a network of hydrogen bonds, and therefore its role as ”mediator” for such a rotation-like movement of the bicarbonate ligand might be questionable. In order to estimate the mobility of the water molecule during this rearrangement an animation of the complete reaction sequence shown in Figure 3 is given in Video 2. From this, one can see that the position of the water molecule is not influenced significantly during the rotation-like movement and thus this ”deep” water molecule should indeed be able to mediate this reaction and - at the same time – maintain a hydrogen bond network.

In order to simulate a Lipscomb-like mechanism within this model system, a suitable transition state structure must involve the active site water molecule acting as a proton shuttle between the zinc-bound oxygen (H-donor) and “free” HCO_3^- oxygen (H-acceptor). However, a geometry for such a transition state that meets all the requirements mentioned above could not be found. Instead, our energy surface scans for an appropriate internal proton transfer invariably led to the transition state **8TS2.**

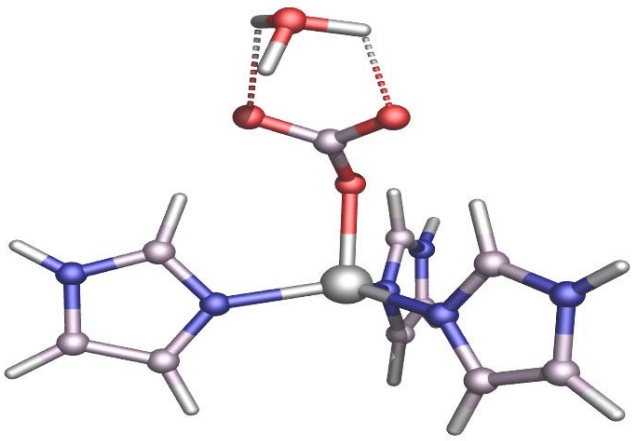

Although an H_3O^+ ion acts as a proton shuttle in this structure, it does not transfer the proton between zinc bound and the “free” HCO_3^- oxygens but rather between two “free” oxygens. Therefore, **8TS2** is not a model for the conversion of reactant **8** into product **9** by means of an internal proton transfer. However, **8TS2** allows us to estimate the energy barrier for an internal proton transfer within this model system. The calculated heat of formation (Table 1) for transition state **8TS2** is 110.3 kcal·mol^{-1}, 20.9 kcal·mol^{-1} higher then that for the alternative transition state **8TS**, supporting a Lindskog-like mechanism**.** Comparison with the energy barrier of 0.4 kcal·mol^{-1} for the rotation-like movement of the bicarbonate ligand, makes a Lipscomb–like mechanism unlikely.

The {[Im$_3$ZnOH]$^+$·H$_2$O·CH$_3$OH·CO$_2$} active site model complex

In order to enhance the model system for HCAII further, a model for the mechanistically important Thr-199 side chain was added to the {[Im$_3$ZnOH]$^+$·H$_2$O·CO$_2$} active site model complex in the form of a methanol molecule. Figure 4 summarises the structures obtained for the interaction between water, carbon dioxide, methanol and **1**. The formation of van der Waals–complex **11** leads to a gain in energy of –14.7 kcal·mol^{-1} and is therefore more exothermic than the second model system (Figure 3) by 2.3 kcal·mol^{-1}. This is due to a more extensive hydrogen bond pattern, which now also involves a hydrogen bond between an imidazole hydrogen and methanol. The r(CO···Zn) distance was calculated to be 4.39 Å, whereas r(C···OZn) is 2.34 Å. Further approach of CO_2 to the active site complex {[Im$_3$ZnOH]$^+$·H$_2$O·CH$_3$OH}, yields the transition state structure **11TS** and finally results in the formation of the *precursor* bicarbonate complex **12**. The energy of activation on going from **11** to **12** was calculated to be 3.0 kcal mol^{-1}, whereas the total reaction energy is –3.2 kcal·mol^{-1}. Compared to the analogous reaction from **7** to **8**, this reaction has a lower barrier by 0.3 kcal·mol^{-1}, but is more endothermic by 0.8 kcal·mol^{-1}. The r(CO···Zn) and r(C···OZn) distances in transition state **11TS** were calculated to be 3.81 Å and 1.83 Å, respectively, thus showing again that there is no tendency for direct CO_2 coordination to the Zn^{2+} during nucleophilic attack of zinc bound hydroxide on the CO_2 carbon. Further rearrangement of the HCO_3^- ligand *via* a Lindskog-like mechanism results in the formation of transition state **12TS,** which is higher in energy than its *precursor* bicarbonate complex **12** by only 0.1 kcal·mol^{-1}. Although, this small energy barrier is well beyond the accuracy of AM1, it is the only transition state structure found for the formation of the final, energetically most stable bicarbonate complex **13**. Again, no evidence for an internal proton transfer was found and attempts to localise an analogue to **8TS2**, which would at least allow the estimation of the energy of activation for such a process, invariably lead to **12** or **13**. The overall reaction energy on going from **12** to **13** is calculated to be –12.3 kcal·mol^{-1}, making this the most exothermic bicarbonate formation reaction found for all three model systems. Therefore, we conclude that this model system is most reasonable for simulating enzymatic catalysis of HCAII, and that the overall mechanism for the formation of the bicarbonate ion is best described as an initial nucleophilic attack of CO_2 by zinc bound hydroxide, followed by a Lindskog-like rearrangement of the bicarbonate ligand.

Conclusions

Semiempirical AM1 calculations applied to selected active site model systems for HCAII and their reaction with the substrate CO_2 show a strong dependence of the preferred mechanism for the formation of a bicarbonate complex on the size of the model used. On going from the

{[$Im_3ZnOH]^+ \cdot CO_2$} active site model to the more sophisticated model systems {[$Im_3ZnOH]^+ \cdot H_2O \cdot CO_2$} and {[$Im_3ZnOH]^+ \cdot H_2O \cdot CO_2 \cdot CH_3OH$}, in which additional "deep" water and Thr-199 side chain are considered, the change from the Lipscomb-like mechanism (internal proton transfer) towards a Lindskog-like (rotation-like) formation of the final bicarbonate complex is observed. Beside the structural alterations shown by means of the selected structural parameters r(CO···Zn) and r(C···OZn), increasing the size of the model gives a decrease in the calculated energy of activation. The highest energy barrier for the overall internal proton transfer mechanism is 36.8 kcal·mol^{-1}, whereas an almost activationless mechanism was found for the rotation-like rearrangement of the HCO_3^- ligand. Although the model systems under investigation differ in their mechanistic details for the bicarbonate formation, they all agree in that the direct coordination of CO_2 oxygen to Zn^{2+} does not occur in the initial reaction step. Thus, we conclude that within these model systems and the level of theory applied, a nucleophilic attack of zinc bound hydroxide on CO_2 carbon followed by a Lindskog-like formation of the bicarbonate complex are preferred.

We are aware of the fact that the level of theory leads to limitations in the prediction of the reaction mechanism of HCAII and that neglecting a large part of the enzyme might effect the obtained results. Thus, our further investigations of this enzyme catalysis will involve density functional theoretical approaches based on the structures presented in this paper and more complete active site models. However, the calculated modes of action of HCAII, CPA [20a] and LADH [20b] present a consistent picture of a general base-type mechanism in monozinc enzymes, so that we do not expect any surprises from further studies. Binuclear zinc and zinc/calcium enzymes, [31] however, present an interesting extension of the type of studies presented here and may reveal new mechanistic features. More extensive calculations including solvent effects (SCRF and molecular dynamics) will be used to investigate the overall stability, especially of the proposed van der Waals complexes.

Acknowledgements The authors gratefully acknowledge financial support from the Deutsche Forschungsgemeinschaft and helpful discussions with Arieh Warshel.

Supplementary Material available statement The reactions shown in the various Figures are animated as Autodesk Animations (*.flc) [30]. The Animation files are: Video1.flc, which involves the reactions shown in Figures 1a and 2. Video2.flc, which is an animation of the reaction shown in Figure 3. Video3.flc is an animation of the reaction shown in Figure 4.

References

1. For a selection of reviews see: (a) Silverman, D.; Vincent, S. H. *CRC Crit. Rev. Biochem.* **1983**, *14*, 207. (b) Bertini, I.; Luchinat, C. *Acc. Chem. Res.* **1983**, *16*, 272. (c) Coleman, J. E. In *Zinc Enymes*; Bertini, I., Luchinat, C., Maret, W.,Zeppezauer, M., Eds.; Birkhäuser: Boston, 1986; p49. (d) Silverman, D. N.; Lindskog, S. *Acc. Chem. Res.* **1988**, *21*, 30. (e) Dodgson, S. J.; Tashian, R. E.; Gros, G.; Carter, N. D. *The Carbonic Anhydrases*. Plenum press: New York, 1991. (f) Christianson, D.W.; Fierke, C. A. *Acc. Chem. Res.* **1996**, *29*, 331.
2. Lindskog, S. In *Zinc Enzymes*; Spiro, T. G. , Ed.; Wiley: New York, 1983; p77.
3. (a) Lipscomb, W. N. *Ann. Rev. Biochem.* **1983**, *52*, 17. (b) Liang, J.-Y.; Lipscomb, W. N. *Biochemistry* **1987**, *26*, 5293.; **1988**, *27*, 8676.
4. Silverman, D. N.; Rowlett, R. S. *J. Am. Chem. Soc.* **1982**, *104*, 6737.
5. (a) Tashian, R. E. *Adv. Genet.* **1982**, *30*, 321. (b) Hewett-Emmett, D.; Tashian, R. E. *Mol. Phylogenet. Evol.* **1996**, *5*, 50.
6. Eriksson, A. E.; Jones, A. T.; Liljas, A. *Proteins* **1988**, *4*, 274.
7. Xue, Y.; Liljas, A.; Jonsson, B.-H.; Lindskog, S. *Proteins* **1993**, *17*, 93.
8. Merz, K. M., Jr.; Hoffmann, R.; Dewar, M. J. S. *J. Am. Chem. Soc.* **1989**, *111*, 5636
9. (a) Davis, R. P. J. *Am. Chem.Soc.* **1959**, *81*, 5674. (b) Coleman, J. E. *J. Biol. Chem.* **1967**, *242*, 5212.
10. Liang, J.-Y.; Lipscomb, W. N. *Int. J. Quantum. Chem.* **1989**, *36*, 299.
11. Jacob, O.; Cardenas, R.; Tapia, O. *J. Am. Chem. Soc.* **1990**, *112*, 8692.
12. (a) Krauss, M.; Garmer, D. R. *J. Am. Chem. Soc.* **1991**, *113*, 6426. (b) Garmer, D. R.; Krauss, M. *J. Am. Chem. Soc.* **1992**, *114*, 6487.
13. Zheng, Y.J.; Merz, K. M., Jr. *J. Am. Chem. Soc.* **1992**, *114*, 10498.
14. Nair, S. K.; Christianson, D. W. *Eur. J. Biochem.* **1993**, *213*, 507.
15. Zhang, X.; van Edlik , R. *Inorg. Chem.* **1995**, *34*, 5606.
16. Zhang, X.; Hubbard, C. D.; van Eldik, R. *J. Phys. Chem.* **1996**, *100*, 9161.
17. Hartmann, M.; Clark, T. van Eldik, R. *J. Mol Model.* **1996**, *2*, 358.
18. Merz, K. M., Jr.; Banci, L. *J. Am. Chem. Soc.* **1997**, *119*, 863.
19. Garmer, D. R. *J. Phys.Chem.* **1997**, *101*, 2945.
20. (a) Alex, A.; Clark, T. *J. Comput.Chem.* **1992**, *13*, 704. (b) R. von Onciul, A.; Clark, T. *J. Comput.Chem.* **1993**, *14*, 392.
21. Nair, S. K.; Calderone, T. L.; Christianson, D. W.; Fierke, C. A. *J. Biol. Chem.* **1991**, *266*, 17320.
22. Dewar, M. J. S.; Zoebisch, E. G.; Healy, E. F.; Stewart, J. J. P. *J. Am. Chem. Soc.* **1985**, *107*, 3902.

23. Clark, T.; Alex, A.; Beck, B.; Chandrasekhar, J.; Gedeck, P.; Horn, A.; Hutter, M.; Rauhut, G.; Sauer, W.; Steinke, T. **VAMP 7.0** Oxford Molecular Ltd., Medawar Centre, Oxford Science Park, Sandford-on-Thames, Oxford, OX4 4GA, Great Britain..
24. Merz, K. M., Jr.; Dewar, M. J. S. *Organometallics,* **1988**, *7*, 522.
25. Baker, J. *J. Comput. Chem.* **1986**, *7*, 385.
26. *Non-linear Optimization*; Powell, M. J. D , Ed.; Academic Press: New York, 1982.
27. Fletcher, R. *Practical Methods of Optimization*, Wiley: Chichester 1981.
28. Dewar, M. J. S.; Kirschner, S. *J. Am. Chem. Soc.* **1971**, *93*, 4290.
29. (a) Gonzales, C.; Schlegel, H. B. *J. Chem. Phys.*, **1989**, *90*, 2154; *J. Phys. Chem.*, **1990**, *94*,5523.
30. Copyright of the various programs used for the creation of the animation sequences is owned by: Dr. Jeffrey J. Gosper, Brunel University for the program suite Re_View2 (1997); the POV-Ray Team for the ray tracing program POVRay 2.0 (1993); David K. Mason for his TGA-Animation Program (1991-1993), and Autodesk Inc. for the Autodesk Animator Windows Player 1.0 (1990-1991). All programs were used in their freeware/shareware versions distributed via Internet.
31. Schürer, G.; Clark, T. *J. Chem. Soc., Chem. Commun.*, **1998**, 257.